Spectroscopic Assessment of Biomass Derived Adsorbents for Oil Spill Cleaning

Christina G. Siontorou[1], Maria Bidikoudi[2], Chryssa Chandrinou[2], Nikos Boukos[2], Polycarpos Falaras[2], Michael Fardis[2], George Apostolopoulos[3], Fragiskos Batzias[1] and Dimitris Sidiras[1]

***Abstract*—**Lignocellulosic residues from fibrous agricultural crops present a low-cost, environmental-friendly, and readily available feedstock to produce sorbents for oil spill cleaning, either in marine or fresh water environment. Owing to the complex and packed structure of lignocellulose, pre-treatment has a critical role to play in converting biomass to a high efficient sorbent for oils. This work compares the efficiencies of sulfuric acid and maleic acid treatment on the adsorptivity of wheat straw, using FTIR spectroscopy, micro-Raman spectroscopy, NMR and BET analysis. The results indicate that maleic acid has more profound effect on both, the exterior and the interior cell wall layers, expressed as enhanced adsorptivity for oils.

***Keywords*—** Crude oil adsorption, diesel adsorption wheat straw, maleic acid pretreatment, sulfuric acid pretreatment

I. Introduction

RENEWABLE biomass presents a low-cost, environmental-friendly, and readily available feedstock to produce efficient sorbents for oil spill cleaning, either in marine or fresh water environment. Oil removal is based on adsorption, i.e., the attraction and adhesion of oil to the surface of the sorbent [1]; attraction proceeds via chemical (covalent or hydrogen bonding), electrostatic (ion–ion or ion–dipole interaction), and physical (Coulombic, Kiesom energy, Debye energy, London dispersion energy) forces. Process efficacy depends on material adsorptivity that tends to be higher for porous structures [2]. Apart from morphology, several studies have shown that oil adsorption is governed by the functional group properties of the sorbent [3-6]; better adsorptivity lies within O-H, C-O and C=O groups.

Lignocellulosic residues from fibrous agricultural crops seem more promising, owing to their micro- and macro-porous structures that permit oil attachment and entrapment [7-9]. Despite, the complex structure of lignocellulose renders the biomass-to-sorbent conversion neither straightforward nor equally applicable or successful to all types of agricultural waste. Cellulose microfibers are embedded in a matrix of biopolymers, primarily hemicellulose and lignin (Fig. 1). The outer protective layer is held in place by an intertwining network of ether- and ester-bonds between lignin and hemicellulose [10]. The interior cellulose layer is tightly packed, practically impenetrable to even low molecular weight solutes, such as water [10]; some parts, however, of the fibril layer are less ordered, almost amorphous (Fig. 2). This arrangement allows for van der waals forces to carry the adsorption process (physisorption),

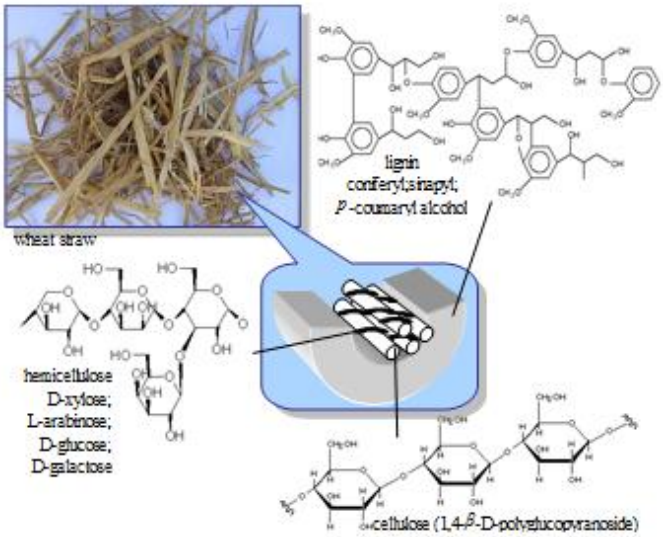

Fig. 1 Simplified representation of wheat straw structure: lignin accounts for 14%-18% of the dry mass, inter-linked to celluloses and hemicelluloses with a network of ether- and ester-bonds.

Christina G. Siontorou, Fragiskos Batzias and Dimitris Sidiras[1] are with the Department of Industrial Management and Technology, School of Maritime and Industry, University of Piraeus, 80 Karaoli and Dimitriou Str., GR18534, Piraeus, Greece.

Maria Bidikoudi, Chryssa Chandrinou, Nikos Boukos, Polycarpos Falaras and Michael Fardis[2] are with the Institute of Nanoscience and Nanotechnology, National Centre for Scientific Research "Demokritos", GR15310 Agia Paraskevi Attikis, Athens, Greece..

George Apostolopoulos[3] is with the Institute of Nuclear & Radiological Sciences and Technology, Energy & Safety (INRASTES), National Centre for Scientific Research "Demokritos", GR15310 Agia Paraskevi Attikis, Athens, Greece.

This research has been co-financed by the European Union (European Social Fund - ESF) and Greek national funds through the Operational Program "Education and Lifelong Learning" of the National Strategic Reference Framework (NSRF) - Research Funding Program: THALIS - UNIVERSITY OF PIRAEUS - DEVELOPMENT OF NEW MATERIAL FROM WASTE BIOMASS FOR HYDROCARBONS ADSORPTION IN AQUATIC ENVIRONMENTS.

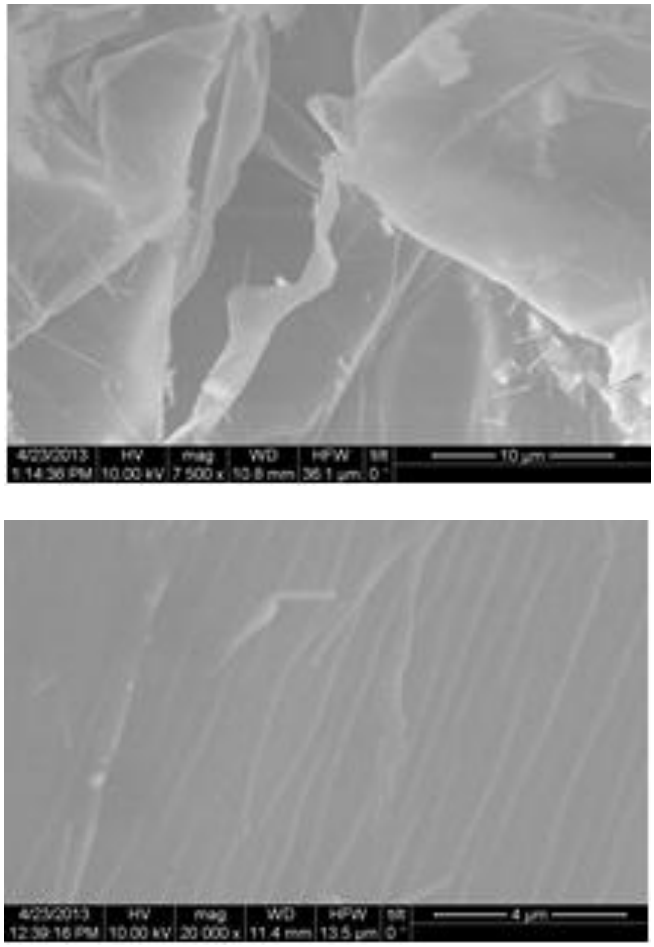

Fig. 2 SEM images for the interior of wheat straw: *x* 7500 magnification (top) and *x* 20000 magnification (bottom).

limiting the availability of covalent bonding (chemisorption). Evidently, the expressed adsorptivity of the raw material may not be adequate to justify its potential, unless its structure is 'opened' to increase surface area and expose the binding sites [11].

Biomass treatment targets the disruption of the lignocellulosic structure, at the extent feasible by the process: physical treatment, i.e., heating/boiling, freezing/thawing, and lyophilization, does not degrade the fibril structure of cellulose but causes lignin re-localization [11]; chemical treatment, involving mostly organic solvents, alkalis or acids, depolymerizes lignin and hydrolyzes hemicellulose [6-8].

The potential of any biomass type to convert to sorbent products can be determined using simulations in batch and/or fixed bed systems that provide (i) comparable estimates for the adsorption capacity of untreated and treated samples, (ii) some insights on the impact of treatment on lignocellulose structure (i.e., the extent of disruption), and (iii) certain assumption on the mechanisms involved in adsorption [2-9]. The elucidation, however, of these mechanisms is required for treatment evaluation, sorption optimization, and the scale-up of both, process and product [10,11]. Reversibility of the process is, also, an issue to consider [7]. In effect, as disruption propagates to the cellulose framework, sorption phenomena become irreversible [10]. In oil spill management, oil recovery (desorption) is crucial. Oil is regarded as a precious commodity; further to the environmental issues raised, inefficient extraction implies also economic loss. Thus, an efficient sorbent should allow easy and rapid recovery of the adsorbed oil.

Previous studies determined the effect of autohydrolysis [8] and sulfuric acid hydrolysis [9] on the adsorptivity of wheat straw, using BET surface area, scanning electron microscopy (SEM), X-ray diffraction and Fourier transform infrared (FTIR) spectra. The autohydrolysis pretreatment increased the hydrophobicity of wheat straw rendering it more oil-assimilative [8]. The removal, however, of the hemicelluloses and the amorphous celluloses gave rise to a high lignin residual and allowed the degradation of the micro-structure, making the sorbent less floatable. Overall, the product expressed low sorption capacity, quite unsuitable for oil spill cleaning. Mild acid treatment provided better results on sorption capacity, justified by surface area estimations [9]. As the testing system involved dyes, its suitability for oil remains elusive.

This work compares the efficiencies of sulfuric acid and maleic acid treatment on the adsorptivity of wheat straw, using FTIR spectroscopy, micro-Raman spectroscopy, NMR and BET analysis. Oil adsorption has been simulated using crude oil and diesel. Several conclusions on the impact of acids on the lignocellulosic structure have been drawn. The results indicate that maleic acid has more profound effect on both, the exterior and the interior cell wall layers, expressed as enhanced adsorptivity for oils.

II. Methodology

A. Materials and Pre-treatment

The wheat straw used in this work was obtained from the Kapareli village, close to the Thiva city at the Kopaida area in central Greece (harvesting year 2012), as a suitable source for full-scale industrial applications. The moisture content of the material when received was 8.8% w/w; after screening, the fraction with particle sizes between 10 and 20 mm was isolated.

1) Sulfuric acid hydrolysis

The larger particle fraction was treated in CHEMGLASS 20-L glass reactor, whereas a 0.5-L glass reactor was used for the smaller fraction. The solid residue yield was 55.34% w/w on dry basis.

The treatment conditions for the 20-L reactor were: (i) the acid hydrolysis isothermal time was 4 h (not including the preheating time); (ii) the reaction was catalyzed by sulfuric acid 0.45 M at a liquid-to-solid ratio of 20:1; (iii) the liquid phase volume (water) was 10 L and the solid material dose (wheat straw) was 500 g; (iv) the reaction ending temperature was 100 °C reached after the 1 h and 50 min preheating period.

The treatment conditions for the 0.5-L reactor were: (a) the acid hydrolysis isothermal time was 0-4 h (not including the

preheating time); (b) the reaction was catalyzed by sulfuric acid 0.06-1.8 M at a liquid-to-solid ratio of 10:1; (c) the liquid phase volume (water) was 400 mL and the solid material dose (wheat straw) was 40 g; (d) the reaction ending temperature was 100 °C reached after the 40 min preheating period.

2) Maleic acid hydrolysis

The wheat straw was pretreated by hydrolysis catalyzed with maleic acid ($C_4H_4O_4$). The acid hydrolysis process was performed in a 3.75-L batch reactor PARR 4843. The isothermal acid hydrolysis time was 0-50 min (not including the preheating time). Maleic acid concentration varied within 0.01-0.09 M, at a liquid-to-solid ratio of 20:1. The liquid phase volume was 2000 mL, whereas the solid material dose (wheat straw) was 100 g. The reaction ending temperature was 140 °C – 180 °C, reached after the 35 - 50 min preheating time-periods, respectively.

B. FTIR Spectroscopy

IR spectra were collected on a Thermo Scientific Nicolet 6700 FTIR with N_2 purging system. Spectra were acquired using a single reflection ATR (attenuated total reflection) SmartOrbit accessory equipped with a single-bounce diamond crystal (spectral range: 10,000–55 cm^{-1}, angle of incidence: 45°). A total of 32 scans were averaged for each sample and the resolution was 4 cm^{-1}. The spectra were obtained against a single-beam spectrum of the clean ATR crystal and converted into absorbance units. Data were collected in the range 4000–400 cm^{-1}.

C. Micro-Raman Spectroscopy

The Raman spectra of the samples were recorded on a Renishaw inVia Reflex spectrometer in backscattering configuration employing a near infrared (NIR) diode laser (λ=785 nm) as excitation source. Rayleigh scattering was rejected with a 100 cm^{-1} cut-off dielectric edge filter, and analysis of the scattered beam was performed on a 250 mm focal length spectrometer along with a 1200 lines/mm diffraction grating and a high-sensitivity CCD detector. Intensity of laser was set at 0.5 $mW/\mu m^2$. Subtraction of the luminescence background (%) was performed for the wavenumbers range between 120 and 1700 cm^{-1}.

D. Liquid Nitrogen Porosimetry

The surface areas and porosity of the powders were determined by the Brunauer-Emmet-Teller (BET) method. Liquid nitrogen isotherms at 77 K were obtained, using the Autosorb-1 MP (Quantachrome) porosimeter. Before each measurement, the samples were degassed, under high vacuum 10^{-5} mbar for 24 h, at 353K in the outgassing stations of the instrument. The selected program of relative pressures covered all the pore sizes from the ultra-micropore to the large mesopores region ($1x10^{-5}$<=P/Po<1).The tolerance and equilibration time of all the pressure points were set to 0 and 10 respectively. Before performing the measurements, all samples were turned into powders using a hummer mill.

E. Nuclear Magnetic Resonance

Untreated and treated wheat straw samples were immersed in crude oil and diesel simulated water spill, according to ASTM F 726: Standard Test Method for Sorbent Performance of Adsorbents (2012). After drying, the samples were immersed in a pyrex glass and rinsed with distilled water, in order to increase the water content of the pores. The pyrex glass was then put into a desiccator and subsequently pumped with a mechanical pump at a vacuum pressure of ca. 0.1 mbar for 90 min.

III. Results and Discussion

A. Sulfuric Acid Treatment

Comparing the FTIR spectra from the raw and pretreated materials (Fig. 3), the most important changes concern the intensity of peaks and bands and refer mostly to the breakdown of lignin and transformation of cellulose to a more amorphous phase. Some new peaks appear, attributed to the formation of bonds between sulfur (S) and oxygen (O_2).

In the region between 4000 and 3000 cm^{-1} there is a strong band between 3500-3100 cm^{-1} assigned to OH stretching vibrations, which is a band present in every lignin IR spectrum. It is caused by the presence of alcoholic and phenolic hydroxyl groups involved in the hydrogen bonds. This band, appearing in both, treated and untreated samples, indicates the presence of lignin. No alteration is observed in neither the position nor the intensity of the band, suggesting that H_2SO_4 does not affect the lignin content.

Two peaks appear at the spectra of untreated wheat straw in the region of 3000-2500 cm^{-1}, at 2918 and 2850 cm^{-1}, caused by the asymmetric and symmetric stretching of methylene and ethylene ($-CH_2-$) groups in long alkyl chains. This peak suggests the presence of waxes; similar impurities have been, also, identified in previous studies [12]. These peaks remain unchanged after the H_2SO_4 treatment.

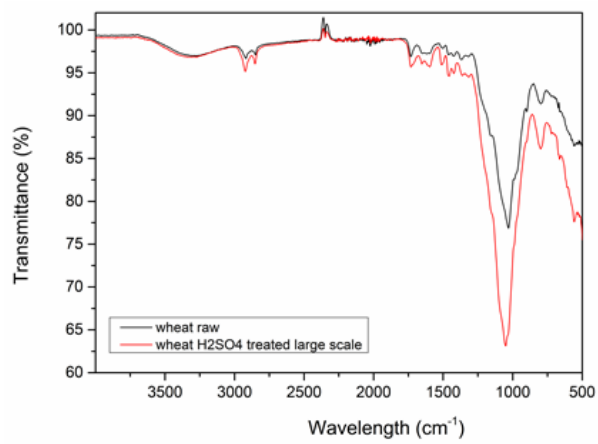

Fig. 3 FT-IR spectra of untreated (black line) and sulfuric acid treated (red line) wheat straw

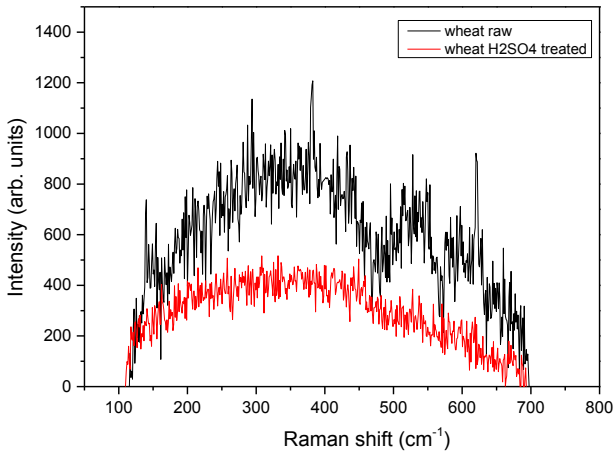

Fig. 4 Micro-Raman spectra of untreated (black line) and sulfuric acid treated (red line) wheat straw

Peaks at the region of 2500-2000 cm^{-1} appear due to the roughness of material surface and provide no real information about the samples. In general, bands in the region 1760-1640 cm^{-1} are carbonyl bands (C=O). Carbonyls involve several functional groups, each on a specific wavenumber that permits identification. In both, treated and untreated material, the band appears at 1730 cm^{-1}, a wavenumber accommodating ester functional group. However, the band at ~1720 cm^{-1}, when considered with the weak W-shaped peak between 2850-2750 cm^{-1} indicates the C=O of aldehyde. Treated samples exhibit a band at 1510 cm^{-1}, which is the amide II band; this band is caused by the C-N stretching vibration, in combination with N-H bending and reports on protein unfolding.

Peaks around 1482 cm^{-1} are attributed to CH_3CH_2 and, also, to C=O and C-O of carbonates. Sulfuric acid does not affect these bonds. Peak at 1460 cm^{-1}, attributed to CH_2 scissors vibration and CH_3 antisymmetric deformation, is present in the spectra of both samples, although more intense in the treated sample. This peak is assigned to lignin [13], whereas the transmittance, at 1420 cm^{-1}, is attributed to amorphous and crystalline cellulose [14]. The changes of these bands can be explained by an increase in the rate of crystalline cellulose accompanied by a decrease in the amorphous cellulose area [14]. Peaks at 1398 cm^{-1} are attributed to C-N group, while a symmetric 'doublet' with medium intensity at around 1370 cm^{-1} is characteristic for an isopropyl group. The peaks around 1029 and 1033 cm^{-1} can be assigned to C-O groups in the primary alcohols of lignin [15], while the peak at 1053 cm^{-1} denotes the presence of the glucose ring and sucrose. The 23 cm^{-1} shift (from 1030 to 1053 cm^{-1}) observed in the treated sample indicates that after the treatment, monosaccharides, such as glucose, are combined forming the disaccharide sucrose.

Peak at 897 cm^{-1} corresponds to cellulose; it refers to the sugar ring tension and decreases with increasing severity of treatment, which is consistent with ring opening [16]. There appears a band that corresponds to amorphous cellulose at 798 cm^{-1}. The pre-treated sample exhibits this band at a higher intensity, implying a more amorphous cellulose layer [17]. Bands that appear at 558 and 665 cm^{-1} of the pretreated samples are attributed to $S=(O_2)$ rock mode of sulfur bonds with oxygen, originating from the H_2SO_4 treatment.

The micro-Raman spectra shown in Fig. 4 have been processed to remove background noise. The high level of luminescence that both samples presented detracts from the value of information. At both samples, lignin is present at bands 1,600 and 1,650 cm^{-1}, whereas cellulose gives the bands at 380, 1,098, and 2,900 cm^{-1} [15]. A noticeable difference refers to the number of peaks: the treated sample does not present as many peaks as the untreated one, implying that wheat straw becomes more amorphous after the treatment.

B. Maleic Acid Treatment

A three-parameter experimental design has been used to study the effect of maleic acid: acid concentration, temperature and hydrolysis time (Table I). The FTIR spectra are presented in Fig. 5. The peaks at around 3400 cm^{-1} correspond to O-H stretching band, which is due to the vibrations of the hydrogen-bonded hydroxyl group, whereas those around 3000 cm^{-1} are due to stretching of C-H [18]. These peaks appear in all samples, with or without treatment. The hydrophilic tendency of wheat is reflected in the broad absorption band in the 3700-3100 cm^{-1} region, which is related to the –OH groups present in the main components [19].

TABLE I
CHARACTERISTICS OF WHEAT STRAW TREATED AND UNTREATED SAMPLES

Sample	Maleic acid (M)	Temperature (^oC)	Hydrolysis time (min)
A1	-	-	-
B1	0.01	160	0
B2	0.01	180	25
B3	0.01	160	50
B4	0.05	140	0
B5	0.05	140	50
B6	0.05	180	50
B7	0.09	140	25
B8	0.09	160	50

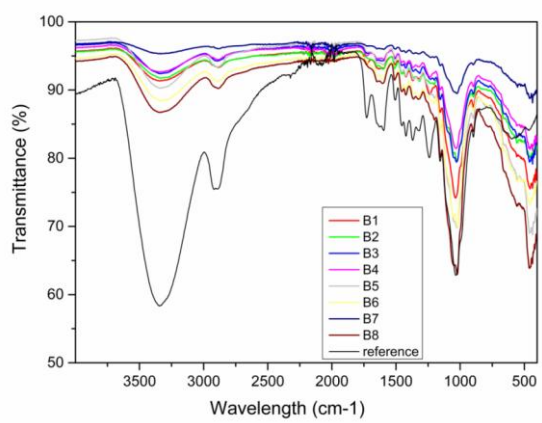

Fig. 5 FT-IR spectra of untreated (reference: A1) and maleic acid treated (samples B1-B8) wheat straw; description of the sample characteristics are provided in Table I

The peak at 1700 cm^{-1} in the reference (untreated wheat straw) may be attributed to either the acetyl and uronic ester groups of the hemicelluloses or the ester linkage of the carboxylic group in the ferulic and *p*-coumaric acids of the lignin and/or hemicelluloses [20]; the disappearance of this

peak after treatment regardless the conditions suggests that most of the hemicellulose is removed by maleic acid.

The peaks in the region of 1200-1060 cm^{-1}, which are also present in all samples, represent the C-O stretch band and deformation bands in the cellulose, lignin and residual hemicellulose [21]. Furthermore, the peaks at 898 cm^{-1} in all samples are assigned to cellulose, due to β-glycosidic linkages of the glucose ring [20]. The peaks between 1536-1543 cm^{-1} are attributed to C-N stretching or N-H stretching of amide II [22], while the peaks at 1440-1450 cm^{-1} are assigned to the aliphatic part of lignin [23].

Every lignin IR spectrum has a strong wide band between 3500-3100 cm^{-1} assigned to OH stretching vibrations. This band is caused by the presence of alcoholic and phenolic hydroxyl groups involved in hydrogen bonds. This band is gradually vanished from the spectra as temperature and hydrolysis time increases, indicating that maleic acid treatment leads to –OH removal (dehydration of samples). Similar effects are observed for peaks between 2800 and 3300 cm^{-1}, due to hydrocarbons and C-H stretching vibrations; the hybridization of the carbon affects the exact position of the absorption — stiffer bonds vibrate at higher frequencies. The gradual disappearance of this band suggests that the lignocellulose decomposition products do not present IR active modes in that region.

The C=O stretching of aldehyde groups disappears in almost all treated samples. The peak at 1690 cm^{-1}, associated with the C=O stretching of primary amide, is eliminated in samples B6, B7, and B8, indicative of the effect of high maleic levels or harsh treatment conditions. Milder conditions (samples B1-B5) exhibit much lower intensity. The presence of the other prominent absorbance at 1535 cm^{-1} may be due to the N–H stretching vibration of amide II linkages of polypeptides or proteins. This peak exists in all samples, indicating that maleic acid does not impose any alterations on this bond. At treated samples, there appears a shift of 10 cm^{-1} of the 1504 cm^{-1} peak of C=C aromatic ring, a shift of 6 cm^{-1} of the $–CH_2$ bending and a shift of 6 cm^{-1} of the -OH bending. Peaks at 1459 cm^{-1}, 1443 cm^{-1}, 1397 cm^{-1}, 1369 cm^{-1}, and 1347 cm^{-1} remain unaltered. The most prominent peak at 1424 cm^{-1}, which is the characteristic band of crystalline cellulose I remains intact, showing that maleic acid does not affect crystalline cellulose. The last shift observed in that range is the shift of C-O phenolic group, by 5 cm^{-1}, at 1292 cm^{-1}.

The most prominent change in the region of 1250-1000 cm^{-1} is the new peak that appears at 1037 cm^{-1} for samples B3, B6 and B8, which corresponds to C-OH peak, attributed to carbohydrate signals [24]. This is in total agreement with the losses of the –OH band at 3000-4000 cm^{-1} and the hydrocarbons at 3000-2500 cm^{-1}. This result indicates that, after maleic acid treatment, the bonds of C-O-H are very much weakened and dissociated at prolonged treatment periods.

The crystallinity index of cellulose, also called the lateral order index (LOI) was calculated as the absorbance ratio of the bands around 1424 and 897 cm^{-1} [25]. All samples present similar LOI values (Table II), indicating a similar degree of crystallinity and an ordered cellulose structure, suggesting that maleic acid treatment has no effect on the degree of crystallinity.

TABLE II
CRYTSALLINITY INDICES OF UNTREATED AND TREATED WHEAT STRAW

Sample	Lateral Order Index (LOI)
A1	1.064
B1	1.060
B2	1.036
B3	1.043
B4	1.036
B5	1.075
B6	1.035
B7	1.020
B8	1.064

Porosity has been assessed in three samples, i.e., A1, B2 and B6 (Table III). The BET values range from 0.58 to 12.38 m^2/g with the maximum value being received for sample B2. A larger BET specific area suggests larger pores. Both pretreated samples present a significantly higher BET value compared to the untreated material, confirming that maleic acid treatment successfully increases the porosity of the material. Total pore volume is derived from the amount of vapor adsorbed at a relative temperature close to unity, assuming pores are filled with liquid adsorbate. From the results derived with the BET analysis it is obvious that both treated materials feature larger pores than the raw material, a property that is highly desirable and was the upper goal of the pretreatment. Interestingly, however, the mean pore diameter reduces significantly after treatment. These findings have been also confirmed by NMR (Fig. 6.).

TABLE III
RESULTS DERIVED AFTER BET ANALYSIS OF THE POROSIMETRY VALUES OBTAINED FOR UNTREATED AND TREATED WHEAT STRAW SAMPLES

	BET (m^2/g)	Total Pore Volume - (mL/g)	Mean Pore Diameter –(nm)
A1	0.58	0.006	41.9
B2	12.38	0.058	18.9
B6	7.51	0.052	27.5

IV. CONCLUDING REMARKS

The effect of sulfuric and maleic acid pre-treatment on wheat straw has been studied herein using FT-IR and micro-Raman spectroscopy, verified by BET surface analysis and nuclear magnetic resonance. The results indicate that sulfuric acid does not affect lignin but manages to intensify the amorphous regions of cellulose; chemical degradation is limited to signs of protein unfolding and disaccharide formation. On the other hand, maleic acid has more profound effect, inducing dehydration, removal of hemicelluloses, aldehyde destruction and weakening of the C-O-H bonds. The

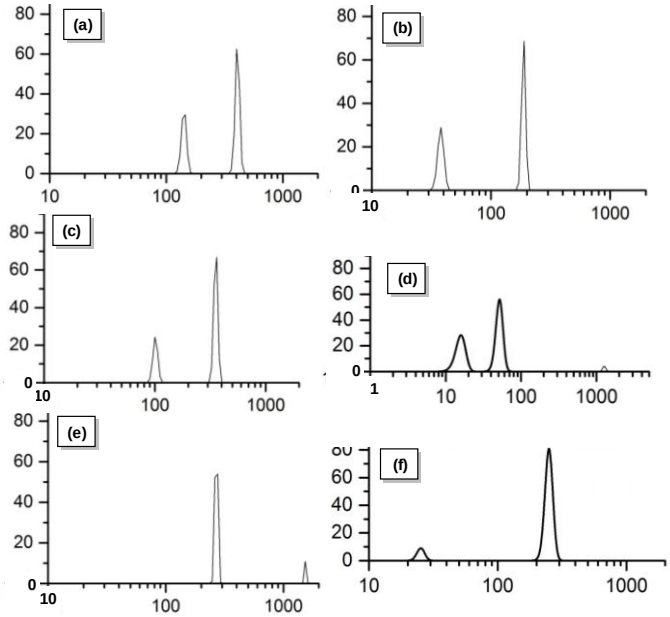

Fig. 6 NMR analysis of untreated (left) and treated (right) wheat straw samples: (a) untreated wheat straw; (b) treated wheat straw; (c) crude oil adsorbed on untreated wheat straw; (d) crude oil adsorbed on treated wheat straw; (e) diesel adsorbed on untreated wheat straw; (f) diesel adsorbed on treated wheat straw.

Porosity of wheat straw is considerably enhanced after treatment, although mean pore diameter is reduced. These findings suggest the superiority of maleic acid treatment for oil adsorption, providing no evidence of covalent bonding at an extent that will hinder desorption.

REFERENCES

[1] M. Schönhoff, "NMR studies of sorption and adsorption phenomena in colloidal systems," *Curr. Opin. Colloid Interface Sci.*, vol. 18, pp. 201-213, 2013. http://dx.doi.org/10.1016/j.cocis.2013.03.004

[2] M. A. Abdullah, A. U. Rahmah, and Z. Man, "Physicochemical and sorption characteristics of Malaysian *Ceiba pentandra* (L.) Gaertn. as a natural oil sorbent," *J. Hazard. Mater*., vol. 177, pp. 683–691, 2010. http://dx.doi.org/10.1016/j.jhazmat.2009.12.085

[3] A. Srinivasan, and T. Viraraghavan, "Oil removal from water using biomaterials," *Bioresour. Technol*., vol. 101, pp 6594–6600, 2010. http://dx.doi.org/10.1016/j.biortech.2010.03.079

[4] E. Khan, W. Virojnagud, and T. Ratpukdi, "Use of biomass sorbents for oil removal from gas station runoff," *Chemosphere*, vol. 57, pp. 681–689, 2004. http://dx.doi.org/10.1016/j.chemosphere.2004.06.028

[5] T. H. Ribeiro, J. Rubio, and R. W. Smith, "A dried hydrophobic aquaphyte as an oil filter for oil/water emulsions," *Spill Sci. Technol. B*, vol. 8, pp. 483–489, pp. 2003.

[6] A. E. A. A. Said, A. G. Ludwick, and H. A. Aglan, "Usefulness of raw bagasse for oil absorption: a comparison of raw and acylated bagasse and their components," *Bioresour. Technol*. Vol. 100, pp. 2219-2222, 2219–2222.

[7] R. Wahi, L. A. Chuah, T. S. Y. Choong, Z. Ngaini, and M. M. Nourouzi, "Oil removal from aqueous state by natural fibrous sorbent: An overview," *Sep. Purif. Technol.*, vol. 113, pp. 51–63, 2013. http://dx.doi.org/10.1016/j.seppur.2013.04.015

[8] D. Sidiras, F. Batzias, I. Konstantinou, and M. Tsapatsis. "Simulation of autohydrolysis effect on adsorptivity of wheat straw in the case of oil spill cleaning," *Chem. Eng. Res. Des.*, vol. 92, pp. 1781–1791, 2014. http://dx.doi.org/10.1016/j.cherd.2013.12.013

[9] F. Batzias, D. Sidiras, E. Schroeder, C. Weber, "Simulation of dye adsorption on hydrolyzed wheat straw in batch and fixed-bed systems," *Chem. Eng. J.*, vol. 148, pp. 459–472, 2009. http://dx.doi.org/10.1016/j.cej.2008.09.025

[10] J. C. del Río, J. Rencores, P. Prensen, Á. T. Martínez, J. Ralph, and A. Gutiérrez, "Structural characterization of wheat straw lignin as revealed by analytical pyrolysis, 2D-NMR, and reductive cleavage methods," *J. Agric. Food Chem*., vol. 60, pp. 5922–5935, 2012. http://dx.doi.org/10.1021/jf301002n

[11] J. B Kristensen, L. G Thygesen, C. Felby, H. Jørgensen, and T. Elder, "Cell-wall structural changes in wheat straw pretreated for bioethanol production," *Biotechnol. Biofuels*, vol. 1, pp. 1-9, 2008. http://dx.doi.org/10.1186/1754-6834-1-5

[12] N. Abidi, E. Hequet,, L. Cabrales, J. Gannaway, T. Wilkins,and LW. Wells, "Evaluating cell wall structure and composition of developing cotton fibers using Fourier transform infrared spectroscopy and thermogravimetric analysis," *J Appl Polym. Sci.*, vol. 107, pp.476-486, 2008. http://dx.doi.org/10.1002/app.27100

[13] D. J. Huang, B. Mu, and A. Q. Wang., "Preparation and properties of chitosan/poly(vinylalcohol) nanocomposite films reinforced with rod-like sepiolite," *Mater. Lett*., vol. 86, pp.69-72, 2012. http://dx.doi.org/10.1016/j.matlet.2012.07.020

[14] X. Colom, F. Carrillo, F. Nogues, and P. Carriga, Structural analysis of photodegraded wood by means of FTIR spectroscopy," *Polym. Degrad. Stab.*, vol. 80, pp.543-549, 2003. http://dx.doi.org/10.1016/S0141-3910(03)00051-X

[15] L. M. Matuana, S. Jin, and N. M. Stark, "Ultraviolet weathering of HDPE/wood-flour composites coextruded with a clear HDPE cap layer," *Polym. Degrad. Stab.*, vol. 96, pp.97-106, 2011. http://dx.doi.org/10.1016/j.polymdegradstab.2010.10.003

[16] B. Esteves, A. Velez Marques, I. Domingos, and H. Pereira, "Chemical changes of heat treated pine and eucalypt wood monitored by FTIR," *Maderas Ciencia y Tecnología*, vol. 15, pp. 245-258, 2013. http://dx.doi.org/10.4067/s0718-221x2013005000020

[17] T. N. Ang , G. C. Ngoh, A. Seak, M. Chua, and M. G. Lee, "Elucidation of the effect of ionic liquid pretreatment on rice husk via structural analyses," *Biotechnol. Biofuels*, vol. 5, pp.67-78, 2012. http://dx.doi.org/10.1186/1754-6834-5-67

[18] A. Kaushik, and M. Singh, "Isolation and characterization of cellulose nanofibrils from wheat straw using steam explosion coupled with high-shear homogenization," *Carbohydr. Res.*, vol. 346, pp.76-85, 2011. http://dx.doi.org/10.1016/j.carres.2010.10.020

[19] L. Cui, Z. Liu, C. Si, L. Hui, N. Kang, and T. Zhao , "Influence of steam explosion pretreatment on the composition and structure of wheat straw," *BioResources*, vol. 7, pp. 4202-4213, 2012.

[20] M. Jonoobi, K. O. Niska, J. Harun, and M. Misra, "Chemical composition, crystallinity, and thermal degradation of bleached and unbleached kenaf bast (*Hibiscus cannabinus*) pulp and nanofibers," *BioResources*, vol. 4, pp. 626-639, 2009.

[21] X. F. Sun, F. Xu, R. C. Sun, P. Fowler, and M. S. Baird, "Characteristics of degraded cellulose obtained from steam-exploded wheat straw," *Carbohydr. Res.*, vol. 340, pp. 97-106, 2005. http://dx.doi.org/10.1016/j.carres.2004.10.022

[22] G. Jagadeesan, A.V. Kavitha, and J. Subashini, "FT-IR study of the influence of *Tribulus terrestris* on mercury intoxicated mice, *Mus musculus* liver," *Trop. Biomed.*, vol. 22, pp. 15-22, 2005.

[23] Z. J. Shi, L. P. Xiao, F. Xu, and R. C. Sun, "Physicochemical characterization of lignin fractions sequentially isolated from bamboo (*Dendrocalamus brandisii*) with hot water and alkaline ethanol solution," *J. Appl. Polym. Sci.*, vol. 125, pp.3290–3301, 2012. http://dx.doi.org/10.1002/app.36580

[24] P. Das, S. Mukherjee, and S. Sen, "Improved bioavailability and biodegradation of a model polyaromatic hydrocarbon by a biosurfactant producing bacterium of marine origin," *Chemosphere*, vol. 72, pp. 1229–1234, 2008. http://dx.doi.org/10.1016/j.chemosphere.2008.05.015

[25] H. Zhao, C. I. L. Jones, G. A. Baker, S. Xia, O. Olubajo, nd V. N. Person, "Regenerating cellulose from ionic liquids for an accelerated enzymatic hydrolysis," *J. Biotechnol.*, vol. 139, pp. 47-54, 2009. http://dx.doi.org/10.1016/j.jbiotec.2008.08.009